Algal Research 84 (2024) 103751

Contents lists available at ScienceDirect

Algal Research

journal homepage: www.elsevier.com/locate/algal

Effects of salinity and temperature on growth performance, biochemical composition, and biosilification process of *Cyclotella cryptica*

Yicun Zhao [a], Yan Sun [a], Zhengfeng Zhu [a], Yuhang Li [b], Lin Zhang [c], Jian Li [d], Spiros N. Agathos [e,f], Chengxu Zhou [a], Jichang Han [a,*]

[a] College of Food Science and Engineering, Ningbo University, Ningbo 315832, China
[b] Laboratory of Marine Organism Taxonomy and Phylogeny, Institute of Oceanology, Chinese Academy of Sciences, Qingdao 266071, China
[c] Key Laboratory of Applied Marine Biotechnology, Ministry of Education of China, Ningbo University, Ningbo 315832, China
[d] School of Biological and Chemical Engineering, Panzhihua University, Panzhihua 617000, China
[e] Earth and Life Institute, Catholic University of Louvain, City Louvain-La-Neuve 1348, Belgium
[f] Qingdao Innovation and Development Base, Harbin Engineering University, Qingdao 266000, China

ARTICLE INFO

Keywords:
Cyclotella cryptica
Salinity
Temperature
Fucoxanthin
PUFAs
Frustule

ABSTRACT

Microalgae are valuable resources for producing high-value compounds, but large-scale cultivation in open raceway ponds (ORPs) faces challenges due to salinity and temperature fluctuations, which affect biomass yield and quality. Developing strains with high productivity and stable quality across varying salinity and temperature levels offers a promising approach to overcoming these challenges. *Cyclotella cryptica*, a marine diatom species, is known for its robustness under diverse salinity conditions, but its biochemical composition and frustule morphology in respond to salinity remains largely unknown. Moreover, the responses of *C. cryptica* to temperature fluctuations are largely unexplored, posing a barrier to its industrial application in ORPs. In this study, *C. cryptica* was cultivated under six salinity levels (19–34 ‰ at 3 ‰ intervals) and five temperature regimes (17–33 °C at 4 °C intervals) to investigate the effects of these environmental factors on growth performance, macronutrient composition, fatty acid (FA) profile, and carotenoid content. Additionally, we examined the biosilica content, frustule morphology, and the transcriptional levels of five frustule biogenesis related genes (*CcSin1*, *CcSin2*, and *CcSAP1–3*) to assess the impact of salinity and temperature on the biosilification process. Our findings revealed that salinity exerts minimal effects on growth, macronutrient composition, FA profile, and carotenoid content, whereas it induces significant variations in frustule morphology and biosilica deposition. In contrast, temperature markedly influences all evaluated parameters. These insights into the adaptive mechanisms of *C. cryptica* to salinity and temperature variations are crucial for optimizing the scale-up cultivation strategy of this species in ORPs.

1. Introduction

Microalgae are increasingly valued for their rapid growth rates, high photosynthetic efficiency, and capacity to produce a diverse range of valuable bioactive compounds. These attributes make them promising resources for industries such as pharmaceuticals, aquaculture feed, and chemical feedstocks [1]. Moreover, microalgae have the unique ability to utilize wastewater and flue gases for cultivation, transforming waste into high-value products [2]. As a result, species such as *Chlorella* spp., *Haematococcus lacustris*, *Phaeodactylum tricornutum*, and *Chaetoceros* spp. are now cultivated on a commercial scale, capitalizing on these advantages [3]. However, the scale-up of microalgae cultivation encounters challenges due to environmental fluctuations, which can significantly impact microalgal yield and quality. Understanding how microalgae respond to various environmental factors is essential for refining cultivation techniques and improving production efficiency and stability.

Salinity and temperature are critical factors that influence the growth and biomass composition of microalgae. For example, Pan et al. explored the effects of various salinity levels (15 ‰–60 ‰) on the growth, photosynthetic activity, and biochemical composition of *Euchlorocystis marina* [4]. They observed that cell density peaked at 15

* Corresponding author.
E-mail address: Hanjichang@nbu.edu.cn (J. Han).

https://doi.org/10.1016/j.algal.2024.103751
Received 30 July 2024; Received in revised form 30 September 2024; Accepted 13 October 2024
Available online 15 October 2024

‰ salinity, reaching 5.0 × 10^6 cells mL^{-1}, which is approximately 1.3 times higher than at 60 ‰ salinity. Furthermore, the highest concentrations of chlorophyll *a*, chlorophyll *b*, and carotenoids were found at 15 ‰, while maximum lipid and polysaccharide contents were noted at 60 ‰ salinity. These findings indicate that lower salinity levels favor the reproduction and growth of *E. marina*, whereas higher salinity levels enhance the accumulation of polysaccharides and lipids. Similarly, Chen et al. investigated the impact of salinity on the lipid composition of *Nitzschia laevis*, finding that high salt concentrations reduced neutral lipids but increased the production of polar lipids such as phospholipids and glycolipids [5]. Notably, the degree of fatty acid (FA) unsaturation increased sharply from 10 to 20 g L^{-1} NaCl but decreased at 30 g L^{-1} NaCl, indicating an adaptive mechanism to maintain membrane stability and function under salt stress. Temperature also significantly affects the quality and yield of microalgal cultivation, as many biological processes in microalgae, including carbon dioxide fixation and respiration, are highly temperature-dependent [6]. Deviations from the optimal temperature range, typically between 20 °C and 30 °C for most microalgae species, can impair or even halt microalgal growth. For instance, *Phaeodactylum tricornutum* exhibits a significantly lower specific growth rate at 25 °C compared to 20 °C, while *Chlorella vulgaris* reaches its maximum growth rate at 30 °C. Similar variations in biomass concentration and biochemical composition in response to salinity and temperature have been reported for various microalgae species, including *C. vulgaris*, *Nannochloropsis* sp., *Isochrysis galbana*, and *Tetraselmis chuii* [7–10]. These studies highlight the importance of salinity and temperature as determinants of microalgal biomass productivity and biochemical composition, emphasizing the need for comprehensive investigations into adaptation strategies to optimize large-scale cultivation systems.

The Open Raceway Pond (ORP), which accounts for approximately 95 % of total industrial microalgal production, is favored for large-scale cultivation due to its cost-effectiveness and high efficiency [11]. However, maintaining optimal salinity and temperature within this system presents significant challenges. Evaporation, a common issue in hot and arid climates, can cause salinity levels to increase, particularly during warm seasons [12]. For instance, in desert regions, daily evaporation rates in an ORP can reach up to 1 cm in depth (approximately 0.2 $L{\cdot}m^{-2}{\cdot}h^{-1}$), potentially doubling the salt concentration of the culture medium within just four days if not replenished with freshwater [4]. This necessitates continuous freshwater addition, significantly increasing water consumption and energy costs. Conversely, rainfall can reduce salinity levels below desirable thresholds. In southern China, for example, salinity in mariculture ponds typically ranges from 25 ‰ to 35 ‰ but can drop below 20 ‰ during the rainy season [13]. Given the shallower depth and larger surface area of ORPs compared to shrimp ponds, the impact of rainfall on salinity reduction is substantially more pronounced in ORPs, often requiring the addition of salt to restore appropriate levels. If not managed, these salinity fluctuations can lead to the dominance of undesirable microalgal strains and a decline in the desired species due to osmotic stress [13]. Temperature control is equally critical in microalgal cultivation due to the temperature sensitivity of these organisms. Non-optimal temperatures can result in significant biomass losses, especially in outdoor systems where daily temperature fluctuations can reach up to 10 °C [3,14]. Engineering solutions such as heating and cooling systems are crucial for maintaining temperatures close to optimal levels in microalgae cultivation. Pérez-López et al. noted that in outdoor facilities, including both photobioreactors and ORPs located in temperate regions (51° 59′ N, 5° 39′ E), temperature control is the primary contributor to energy costs during the scale-up of microalgae cultivation [15,16]. This finding underscores the importance of efficient temperature management in minimizing environmental impacts and operational costs associated with microalgal production.

In addition to engineering approaches such as adjusting salinity with freshwater or salt in ORPs, and modulating temperatures through heating and cooling systems, developing microalgae strains that can produce high biomass across diverse salinity and temperature conditions offers a promising solution to environmental challenges. *Cyclotella cryptica*, a model species of the Bacillariophyta, is rich in carotenoids and polyunsaturated fatty acids (PUFAs), known for their antioxidant, anti-inflammatory, anti-obesity, and neuroprotective properties. The silicified cell wall (frustule) of *C. cryptica* also shows significant potential as a bio-nanomaterial for applications in drug delivery and hemostasis. Notably, although *C. cryptica* is generally known as a marine diatom species, it also has the ability to thrive in freshwater environments [17], demonstrating its robust adaptability to salinity fluctuations when cultivated in ORPs. Furthermore, this microalga and its closely related species have been shown to remain viable across a broad temperature range of 15–35 °C, supporting their potential for commercial applications [18–20]. While previous studies have explored the effects of salinity and temperature on the growth performance of *C. cryptica*, comprehensive information on its cellular responses, including biochemical components, morphological features, and biosilica formation processes under varying conditions, is still limited.

In this study, we assessed the effects of salinity and temperature on *C. cryptica* by analyzing various parameters including cell density, biomass content, and macronutrient composition (carbohydrates, proteins, and lipids). Additionally, we examined the FA profiles, carotenoid content, biosilica content, and morphological characteristics of the frustule. To further investigate frustule biogenesis in response to different salinity and temperature conditions, we analyzed the transcriptional patterns of five genes (*CcSin1*, *CcSin2*, *CcSAP1–3*) encoding silicalemma transmembrane proteins using quantitative reverse transcription-PCR (RT-qPCR). The findings from this research will deepen our understanding of the adaptive responses of *C. cryptica* to salinity and temperature fluctuations and offer critical insights for optimizing large-scale cultivation in ORPs.

2. Materials and methods

2.1. C. cryptica strain and cultivation conditions

The marine diatom species *C. cryptica* used in this study was obtained from the Microalgae Collection Center at Ningbo University. It was cultivated under controlled conditions, maintained at a constant temperature of 25 ± 1 °C and exposed to white fluorescent lighting at an intensity of approximately 45 μmol photons·m^{-2}·s^{-1}, adhering to a 12-h light/dark cycle. The algae were grown in NMB3# medium supplemented with 0.1 mM $Na_2SiO_3{\cdot}9H_2O$ [21], prepared using artificial seawater [22]. The salinity and initial pH of the medium were set to 25 ‰ and 8.0, respectively.

Microalgal cells, pre-cultured to the exponential phase, were inoculated into fresh NMB3# medium at a ratio of 1:9 (*v*/v, algal cultures to fresh medium). To establish a range of salinity conditions, six salinity levels (19, 22, 25, 28, 31, and 34 ‰) were prepared by adjusting the concentration of ultrapure water or NaCl in the artificial seawater. A salinity of 25 ‰ was used as the control treatment. For the temperature experiments, photo incubators (Model GXZ-380B, Jiangnan, China) were set to maintain temperatures of 17, 21, 25, 29, and 33 °C, with 25 °C designated as the temperature of the control group. The design of the temperature and salinity gradients was primarily based on the conditions that microalgae may encounter during cultivation in OPRs, providing relevant information for the cultivation of *C. cryptica* in these systems. All treatments were conducted in 500 mL conical flasks, each containing 200 mL of NMB3# medium. The other cultivation conditions were maintained as described above. During cultivation, the flasks were shaken manually three times daily to prevent the cells from settling at the bottom of the conical flasks.

2.2. Investigation of growth performance

The optical density of microalgal cultures was monitored at 750 nm (OD_{750}) every two days using a Varioskan™ LUX spectrophotometer (Thermo Fisher Scientific, USA) to estimate cell density. The specific growth rate (μ, d^{-1}) was calculated based on OD_{750} using the formula (1):

$$\mu\ (d^{-1}) = (ln\ N_{t1} - ln\ N_{t2})/t_1 - t_2 \quad (1)$$

where t_1 and t_2 represent the start and end times of the cultivation period, respectively, while N_{t1} and N_{t2} indicate the OD_{750} values at these respective times. On the final day of cultivation, 10 mL of microalgal culture was filtered using a pre-weighed Whatman GF/F microfiber filter (pore size 0.7 μm). Then, the filter was rinsed three times with 10 mL of ultrapure water, and subsequently dried in an oven at 60 °C for 48 h to achieve a constant weight. Finally, the dry cell weight (DCW) was determined gravimetrically.

2.3. Determination of macronutrients composition

On the final day of cultivation, microalgal cells were harvested by centrifugation at 3220 ×*g* for 10 min. The cell pellets were washed three times with ultrapure water and then lyophilized for subsequent analyses.

Carbohydrate content was determined using a modified phenol-sulfuric acid method [16]. Initially, 1 mL of an enzyme blend (papain and cellulase in equal proportions) was added to approximately 10 mg of lyophilized microalgal powder. The mixture underwent a series of temperature treatments, starting with a 30-min incubation at 40 °C, followed by a 10-min exposure to boiling water, and a 4-h incubation at 70 °C. Afterward, the mixture was centrifuged at 4 °C and 13,539 ×g for 15 min to separate the supernatant. The supernatant was mixed with 4.5 mL of 95 % ethanol and allowed to stand for 12 h. Following another centrifugation at 4 °C and 13,539 ×g for 15 min, the pellet was resuspended in 2 mL of ultrapure water and vortexed at 1200 rpm for 1 min. After resting at room temperature for 10 min, it was centrifuged once more under the same conditions. The final supernatant was treated with phenol and sulfuric acid, boiled for 20 min, and cooled in an ice bath for 10 min. Absorbance at 490 nm was measured using a Varioskan™ LUX spectrophotometer (Thermo Fisher Scientific, USA). The carbohydrate content was quantified using a glucose standard curve.

Lipid extraction was conducted using a modified chloroform-methanol method [23]. Initially, 25 mg of dried microalgae (W_1) was mixed with 2.5 mL of methanol and 1.25 mL of chloroform. The mixture was homogenized for 15 min and then placed on a shaker for lipid extraction at 200 rpm over 12 h. After extraction, the mixture was centrifuged at 13,539 ×*g* to separate the supernatant, which was then transferred to a clean tube. An additional 2.5 mL of chloroform and 4.5 mL of 1 % NaCl solution were added to the supernatant, followed by vortexing at 1200 rpm for 15 min. After a subsequent centrifugation, the lipid-rich lower phase was decanted into a pre-weighed tube (W_2) and evaporated under a stream of nitrogen gas. The tube was then dried, weighed, and recorded as W_3. Lipid content, expressed in mg per gram of DCW, was calculated using the formula (2):

$$\text{Lipid content}\ (mg\ g^{-1}\ \text{of DCW}) = (W_3 - W_2)/W_1 \times 1000 \quad (2)$$

Protein content was analyzed using a modified Coomassie Brilliant Blue staining method [24]. Approximately 10 mg of microalgal powder was first combined with 2 mL of extraction buffer, which consisted of 50 mM Tris-HCl (pH 7.4), 150 mM NaCl, 1 mM phenylmethylsulfonyl fluoride (PMSF), 1 mM EDTA, and 1 % Triton X-100. The mixture was homogenized for 15 min to extract proteins. After homogenization, the solution was placed in an ice bath for 3 h to enhance protein extraction. The mixture was then centrifuged, and 500 μL of the supernatant was collected. This supernatant was subsequently mixed with 2.5 mL of Coomassie Brilliant Blue reagent. The optical density of the solution was measured at 595 nm (OD_{595}), and the protein content was calculated using a standard curve generated from bovine serum albumin.

2.4. Determination of FA profile and carotenoids content

The extraction of FAs was conducted following a previously described method [25]. Approximately 10 mg of freeze-dried microalgal powder was treated with 3 mL of 2 M KOH in methanol and vortexed vigorously. This mixture was then heated at 75 °C for 30 min. After this period, 1.5 mL of 3 M HCl in methanol was added, and the sample was maintained at the same temperature for an additional 30 min to complete the hydrolysis. Fatty acid methyl esters (FAMEs) were extracted using *n*-hexane. Then, the extracted FAMEs were analyzed in triplicate using gas chromatography–mass spectrometry (GC–MS) on an Agilent Technologies system (Model 8890A-5977B, USA) equipped with a 7963A autosampler and a CD-2560 capillary column (100 m × 0.25 mm × 0.2 μm, CNW, Germany). Pure helium was used as the carrier gas at a flow rate of 0.81 mL min^{-1}. The temperature program initiated at 140 °C for 5 min, followed by a ramp of 4 °C min^{-1} to 240 °C, held for 20 min. FAs were identified and quantified based on their retention times, and data were cross-referenced with the NIST14.L and Wiley7 spectral databases.

Carotenoids were extracted from 5 mg of freeze-dried microalgal powder using a 5 mL solution of chloroform:methanol (1:1, *v*/v) supplemented with 0.1 % butylated hydroxytoluene to prevent oxidation. The mixture was vortexed vigorously for 5 min and then subjected to ultrasonication for 20 min in an ice-water bath to enhance the extraction efficiency. Subsequently, the mixture was centrifuged at 13,539 ×*g* at 4 °C for 5 min. The clear supernatant was then carefully filtered through a 0.22 μm polytetrafluoroethylene filter to remove particulate matter. All procedures were performed under dim light or dark conditions to minimize carotenoid degradation, as recommended in previous studies [25]. Carotenoid analysis was conducted using a high-performance liquid chromatograph (HPLC, 1260 Infinity II, Agilent, Germany). The chromatographic separation was achieved on an Agilent Eclipse XDB-C18 column (250 mm × 4.6 mm, 5 μm) at a flow rate of 0.5 mL min^{-1}. The mobile phase consisted of water (Solution A) and acetonitrile (Solution B). Detection was performed at a wavelength of 450 nm, with the column maintained at a temperature of 25 °C. The injection volume for each sample was 10 μL. Two carotenoids (fucoxanthin and diadinoxanthin) were identified and quantified using commercially available standards (Sigma, USA).

2.5. Investigation of biosilica content and the morphological characteristics of frustules

For the analysis of biosilica content [26], approximately 5 mg of freeze-dried microalgal powder was initially mixed with 1 mL of ultrapure water. This mixture was then heated in a metal bath to 95 °C for 1 h to lyse the cells and prevent intracellular silicates from affecting the results. Following this, the mixture was centrifuged at 13,539 ×*g* for 5 min, and the resultant pellet was resuspended in 1 mL of methanol and left to settle overnight. The suspension was centrifuged again, and the frustules were washed repeatedly with methanol until they appeared colorless. After the methanol was decanted, the frustules were washed thoroughly with 1 mL of ultrapure water and centrifuged once more. The clean frustules were then treated with 1 mL of 0.5 M NaOH and reheated to 95 °C for 1 h to dissolve the biosilica. After cooling, the solution was neutralized with 500 μL of 0.5 M H_2SO_4 and centrifuged. The absorbance of the resulting supernatant at 810 nm was measured using a Microplate Reader (Varioskan LUX, Thermo Fisher Scientific, USA). The OD_{810} was used to quantify the biosilica content, calculated against a standard curve of sodium hexafluorosilicate.

Cells harvested on Day 12 were acidified using concentrated HCl (36 %–38 %) at 100 °C for 20 min, then rinsed with distilled water until

neutral pH was achieved. The pellets were air-dried and mounted on aluminum stubs for examination using a Hitachi S-4800 scanning electron microscope (SEM) (Hitachi, Japan). SEM micrographs were analyzed to determine the following morphological parameters of the frustules using ImageJ software: valve diameter, fultoportula number, fultoportula diameter, costa number, rimoportula number, and cribrum pore number. Additionally, the valve diameter and cribrum pore number were used to calculate the cribrum pore density. Notably, the cribrum pore number was specifically assessed on a quarter of the valve that was free from obstruction by girdle bands or other contaminants, while other parameters were measured across the entire valve.

2.6. Transcriptional patterns of genes related to frustule biogenesis

Microalgal cells harvested on Days 4, 8, and 12 were centrifuged at 3220 ×*g* for 10 min. Total RNA was extracted using the Plant RNA kit (Omega, USA). The integrity of the extracted RNA was assessed via agarose gel electrophoresis, and its concentration was determined based on OD_{230}, OD_{260}, and OD_{280} using a NanoDrop ND1000 spectrophotometer (NanoDrop, USA). After the removal of genomic DNA, cDNA synthesis was carried out using the PrimeScript™ RT Reagent Kit (Takara, China).

RT-qPCR was performed using the Taq Pro Universal SYBR qPCR Master Mix-Q712 (Vazyme, China) following the manufacturer's protocol on a CFX96 Touch (BioRad, USA) to evaluate the expression patterns of five genes (*CcSin1*, *CcSin2*, and *CcSAP1–3*, JGI IDs: g20669.t1, g25218.t1, g14294.t1, g8103.t1, g9622.t1) under varying salinity conditions. *Histone H4* (JGI ID g18763.t1) was used as the internal reference gene for normalizing gene expression via the $2^{-\Delta\Delta CT}$ method. Primer pairs were designed using Primer Premier 5 and are listed in Supplementary Table S1. Prior to RT-qPCR, primer specificity was confirmed by conventional RT-PCR using Es Taq MasterMix (CWBIO, China) under the same reaction conditions.

2.7. Statistical analysis

The morphological properties of the frustules were examined by analyzing 8–11 valves from each treatment. For other parameters such as OD_{750}, DCW, FA profile, carotenoid composition, biosilica content, and transcriptional levels of silicalemma transmembrane proteins, three biological replicates were used. Statistical analyses were conducted using one-way ANOVA at a significance level of 0.05, with post hoc testing performed using the Least Significant Difference (LSD) test to identify significant differences across salinity treatments. Statistical calculations were performed using SPSS Statistics 25.0, and differences were considered statistically significant at $p < 0.05$. All values are presented as mean ± standard deviation (SD).

3. Results and discussion

Fig. 1 provides a comprehensive overview of the impact of varying salinity and temperature on several key biological parameters of *C. cryptica*, including growth performance, macronutrient composition, FA profiles, frustule morphology, and gene expression related to biosilification. In general, temperature changes have a broad and significant effect on *C. cryptica*, substantially influencing all of the aforementioned parameters. In contrast, salinity changes exert relatively smaller effects, primarily affecting specific aspects of frustule morphology and the transcriptional patterns of genes related to biosilica deposition. These findings are explored in more detail in the following sections.

3.1. Effects of different salinities and temperatures on growth performance of C. cryptica

OD_{750} is commonly used to monitor the growth of microalgal cultures. However, it may not accurately reflect growth when variations in cell size and pigment content occur across different salinity levels and temperature conditions. In this study, growth performance was therefore evaluated using a combination of OD_{750}, specific growth rate, and final biomass concentration as more comprehensive indicators.

As depicted in Fig. 2a and Supplementary Table S2, *C. cryptica* maintained similar OD_{750} values across various salinity regimes at all evaluated time points, with final OD_{750} values around 0.15, indicating no significant differences among the groups. Similarly, the specific growth rates were consistent across different salinities, averaging 0.20 d^{-1}, with no significant deviations observed (Fig. 2b). The final biomass concentration, measured as DCW, varied slightly from 0.28 g L^{-1} to 0.31 g L^{-1} across the salinity spectrum, supporting the OD_{750} and specific growth rate findings (Fig. 2c).

Each microalga species exhibits a specific optimal salinity range for achieving maximum growth and biomass concentration. Deviations from this range can lead to biochemical and physiological disruptions, osmotic stress, ion imbalances, and the generation of reactive oxygen species. For the marine diatom *C. cryptica*, our results confirm that it can thrive within a salinity range of 19–34 ‰, showcasing a broad favorable salinity tolerance. This robust adaptability aligns with previous studies, underscoring the huge potential of this microalga for cultivation under varied salinity conditions [27–29]. While marine microalgae can tolerate some degree of salinity variation, it remains relatively uncommon for a species like *C. cryptica* to sustain rapid growth across such a broad salinity range. For instance, the marine diatom *Thalassiosira pseudonana* achieved its highest cell density at a salinity of 25 ‰, whereas both higher (30 ‰) and lower (<20 ‰) salinity levels led to a significant reduction in cell density [30]. Furthermore, studies have shown that marine species such as *Tetraselmis chuii* and *Isochrysis galbana* display growth variations under different salinity conditions, with optimal performance observed within narrower salinity ranges [31].

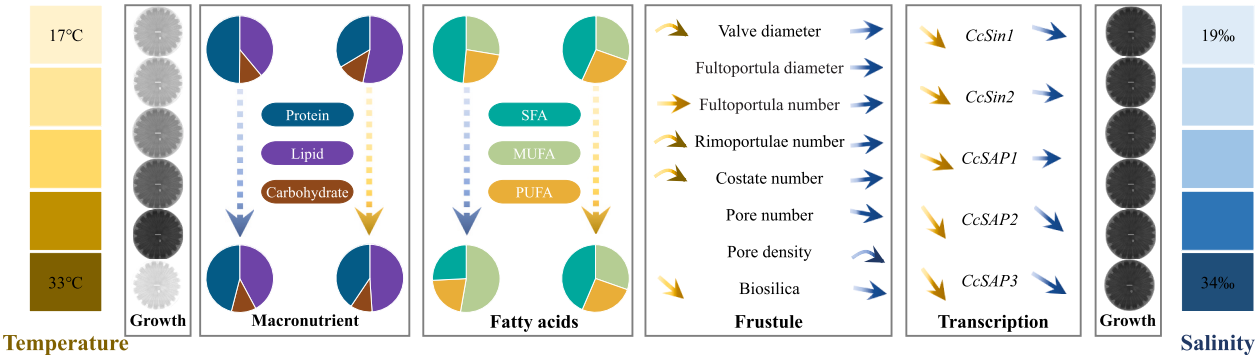

Fig. 1. Summary of the effects of varying salinity and temperature on *C. cryptica*.

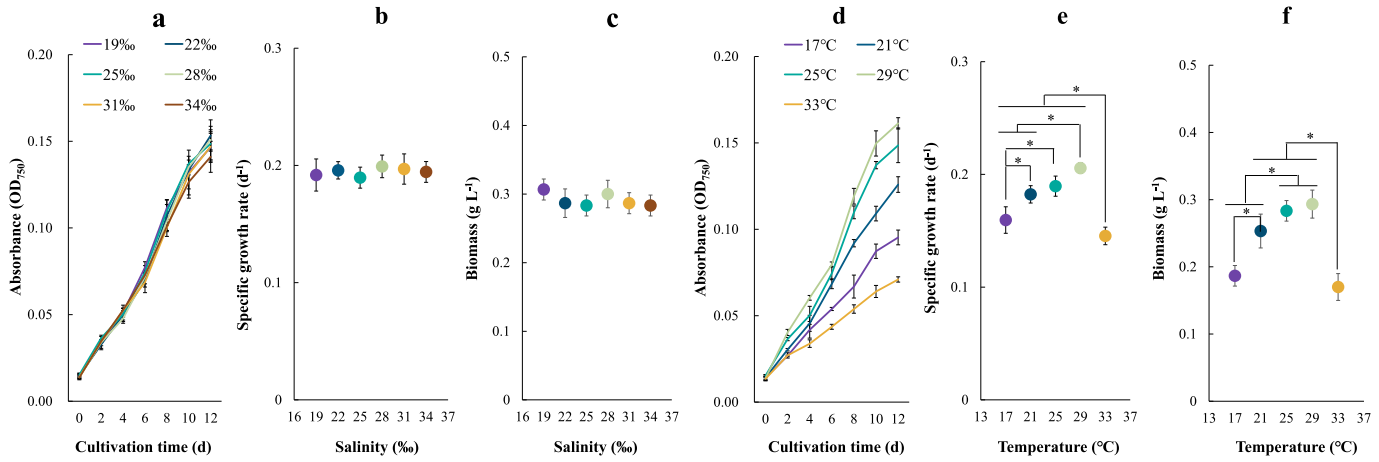

Fig. 2. Cell density, specific growth rate, and biomass concentration of *C. cryptica* cultivated under different salinity levels (a–c) and temperature conditions (d–f). Values are shown as mean ± SD ($n = 3$); * indicates significant differences ($p < 0.05$). The specific growth rate was calculated based on the optical density values from the first and last days of the entire cultivation period.

The mechanisms for coping with salinity variation differ among microalgae species. For example, *Chlamydomonas reinhardtii*, a freshwater species, responds to salt stress by forming multicellular aggregates known as palmelloids, where cells cluster together and are encased within an exopolysaccharide matrix and a common membrane [32]. Marine *Chlorella autotrophica* copes by producing high levels of proline and accumulating inorganic ions to maintain osmotic balance [33]. *Dunaliella* spp., known for their halotolerance, can accumulate substantial amounts of glycerol, up to 17 % of DCW, to preserve cell turgor pressure [34]. Unlike the strategies observed in some Chlorophyta species, the marine diatom *C. cryptica* has been reported to employ two distinct mechanisms to cope with osmotic variations. First, it enhances the biosynthesis of endogenous compatible substances such as dimethylsulfoniopropionate (DMSP), proline, glycine betaine, and taurine. Second, it increases the import of exogenous compatible solutes—such as DMSP, glycine betaine, and amino acids—and potassium, while concurrently exporting sodium [35,36]. These adaptive strategies likely contribute to the capacity of *C. cryptica* to maintain high tolerance under a wide range of salinity conditions, thereby showcasing its robust adaptability to environmental fluctuations.

In contrast to the relatively stable growth observed under varying salinity conditions, changes in temperature had a significant impact on the growth performance of *C. cryptica*. Within the examined temperature range of 17–29 °C, there was a noticeable increase in final OD_{750} values, rising from 0.09 at 17 °C to 0.16 at 29 °C. However, a further increase in temperature to 33 °C resulted in a sharp decrease in OD_{750} to 0.08, essentially halving the value observed at 29 °C (Fig. 2d and Supplementary Table S2). This trend was consistent across other growth metrics as well. The specific growth rate, for instance, peaked at 29 °C with a rate of 0.21 d^{-1}, approximately 1.5 times the rate observed at 33 °C, and showed little variation between 21 °C and 25 °C, maintaining rates of 0.18 d^{-1} and 0.19 d^{-1} respectively (Fig. 2e). Similarly, biomass concentration was highest at 29 °C, reaching 0.29 g L^{-1}, followed by 25 °C at 0.28 g L^{-1}, and 21 °C at 0.25 g L^{-1}. The lowest biomass was recorded at 33 °C, with a concentration of only 0.17 g L^{-1} (Fig. 2f). These observations highlight a critical temperature threshold for *C. cryptica*, beyond which thermal stress adversely affects its cellular processes, leading to decreased growth and biomass production. This temperature-dependent variability underscores the need for controlled cultivation conditions to optimize the growth and yield of this microalga.

While *C. cryptica* has emerged as a well-established model diatom species for biotechnological applications [37,38], its responses to various temperature regimes have rarely been reported. To date, only a few studies have focused on the effects of temperature on the growth performance of this microalga. Sriharan et al. cultivated *C. cryptica* at two temperature levels, 20 °C and 30 °C, and reported significantly higher cell density and biomass concentration at the higher temperature [39]. In another study, Pahl et al. investigated the growth performance of *C. cryptica* within a temperature range of 12.5–33 °C, identifying an optimal temperature range of 22.5–25 °C [28]. However, that study did not explore the effects of temperatures between 25 °C and 33 °C, leaving a gap in understanding the upper temperature tolerance of this species.

In our study, we found that *C. cryptica* can survive within a temperature range of 17–33 °C, identifying a favorable growth range of 25–29 °C. Temperatures exceeding 29 °C or dropping below 21 °C led to considerable inhibition of growth. Although this range appears narrow relative to Chlorophyta species such as *Chlorella* spp. and *Scenedesmus* spp. [40,41], it is broader than that observed for other Bacillariophyta such as *Phaeodactylum tricornutum* and *Thalassiosira pseudonana* [42–44]. Given that the temperature regimes explored in this study closely match the typical range of daytime temperatures across much of the Earth, it suggests that *C. cryptica* may be well-suited for scaled-up cultivation in diverse regions, particularly in temperate zones.

3.2. Biochemical compositions of *C. cryptica* under different salinity and temperature levels

In this study, three major macromolecules in microalgae cells—proteins, carbohydrates, and lipids—along with value-added substances such as FAs and carotenoids were analyzed. Across all six salinity levels tested, *C. cryptica* exhibited the highest concentrations of protein (316.2–343.3 mg g^{-1}), followed by lipid (201.6–262.4 mg g^{-1}), with carbohydrates showing the lowest concentrations (67.5–85.3 mg g^{-1}) (Fig. 3a and Supplementary Table S3). Traditionally, *C. cryptica* is recognized as a significant lipid accumulator, capable of achieving a productivity of 20 $g{\cdot}m^{-2}{\cdot}d^{-1}$ in open raceway ponds (ORPs) [45–47]. However, our results indicated that lipid content was lower than protein content across all salinity conditions tested. This discrepancy may be explained by the fact that the cells analyzed were in the early stationary phase; it is well-documented that *C. cryptica* tends to increase lipid accumulation during the late stationary phase, particularly under nutrient-limited conditions [20].

It is widely known that salinity changes can influence the macromolecular profile of microalgae. Renaud and Parry, for instance, examined the effects of varying salinity levels (10–35 ‰) on the chemical composition of three marine microalgae species—*Isochrysis* sp., *Nannochloropsis oculata*, and *Nitzschia* sp.—noting that lipid contents in *Isochrysis* sp. and *Nannochloropsis oculata* increased with salinity, whereas those in *Nitzschia* sp. decreased [48]. In contrast to these species, *C. cryptica* displayed no significant differences in the concentrations

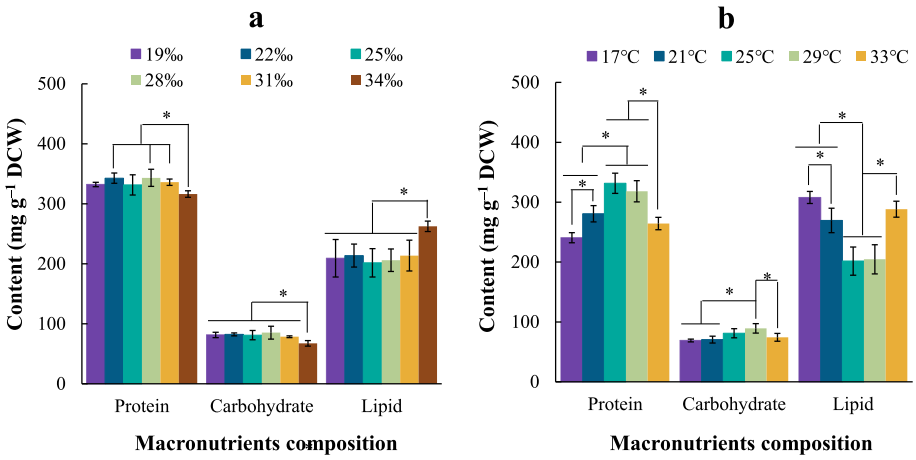

Fig. 3. Macronutrients composition of *C. cryptica* under different salinity (a) and temperature (b) levels. Values are exhibited in mean ± SD ($n = 3$). * indicates significant differences ($p < 0.05$).

of these macronutrients within the salinity range of 19–31 ‰. However, at 34 ‰, both protein and carbohydrate contents were notably lower, while lipid content was significantly higher compared to other conditions. These findings suggest that salinity alterations within the 19–31 ‰ range have minimal impact on the macronutrient composition of *C. cryptica*, but a salinity of 34 ‰ prompts a notable increase in lipid accumulation at the expense of protein and carbohydrate levels.

As illustrated in Fig. 3b and Supplementary Table S3, significant variations in the macromolecular content of *C. cryptica* were observed among different temperature groups. Within the temperature range of 17–25 °C, the protein content showed an increasing trend, rising from 240.7 mg g^{-1} DCW at 17 °C to a peak of 331.4 mg g^{-1} DCW at 25 °C, before gradually declining to 264.4 mg g^{-1} DCW at 33 °C. The carbohydrate content exhibited a similar pattern, initially increasing between 17 °C and 29 °C and then decreasing between 29 °C and 33 °C. In contrast, the lipid content decreased initially from 17 °C to 25 °C but then increased as the temperature rose from 25 °C to 33 °C, displaying a trend opposite to that observed for protein and carbohydrates. Notably, at the extreme temperatures of 17 °C and 33 °C, lipid content was higher than protein content, while at the intermediate temperatures of 21 °C, 25 °C, and 29 °C, protein content surpassed lipid content. This redistribution of cellular carbon flux under temperature stress, from carbohydrate and protein synthesis towards lipid biosynthesis, is a common response among diatoms, as reported in previous studies [49,50]. Our findings corroborate these observations, indicating that lipid content increases while protein and carbohydrate content decrease at the stress-inducing temperatures of 17 °C and 33 °C. This response likely reflects an adaptive mechanism allowing *C. cryptica* to adjust its metabolic pathways to cope with unfavorable thermal conditions.

PUFAs, particularly omega-3 fatty acids such as eicosapentaenoic acid (C20:5, EPA), are valuable compounds prominently present in *C. cryptica*. Slocombe et al. recognized *C. cryptica* as an excellent source for EPA production, ranking it second among 175 microalgal strains from 21 classes [46]. Similarly, Cupo et al. analyzed the FA composition of both autotrophic and heterotrophic *C. cryptica* cultures and noted that EPA, along with palmitic acid (PA, C16:0) and palmitoleic acid (POA, C16:1), dominated the FA profile regardless of the cultivation mode [51].

In this study, we identified a total of 11 FAs in *C. cryptica*, categorized into three saturated fatty acids (SFAs), two monounsaturated fatty acids (MUFAs), and six PUFAs (Tables 1 and 2). Across all six salinity levels, SFAs, MUFAs, and PUFAs constituted 29.7–31.0 %, 25.5–26.6 %, and 42.6–44.1 % of the total fatty acids (TFAs), respectively (Table 1). Interestingly, the concentrations of SFAs, MUFAs, and PUFAs showed no significant variation across different salinities. Consistent with previous findings [46], PA, POA, and EPA were the most prevalent FAs in *C. cryptica*, accounting for 20.2–21.2 %, 19.7–20.7 %, and 17.1–18.5 % of TFAs, respectively. Additionally, hexadecatrienoic acid (HTA, C16:3), hexadecadienoic acid (HDDA, C16:2), and docosahexaenoic acid (DHA, C22:6) were present in moderate amounts, while arachidonic acid (AA, C20:4) and linoleic acid (LA, C18:2) were found in trace quantities (Table 1). Significant differences were noted in the contents of five PUFAs—HTA, LA, AA, EPA, and DHA—across salinity levels (Table 1 and Supplementary Table S4). Notably, DHA content decreased with increasing salinity, from 5.8 % of TFAs at lower salinity levels to 4.6 % at higher levels. HTA content peaked at 31 ‰ (10.7 % of TFAs) but remained relatively stable across the other salinity levels. These findings indicated that while SFAs and MUFAs in *C. cryptica* remain relatively unaffected by salinity, specific PUFAs exhibit significant fluctuations, underscoring the nuanced impact of environmental salinity on the FA biosynthesis of this microalga.

Temperature fluctuations had a more pronounced effect on the FA profile of *C. cryptica* compared to the moderate variations caused by different salinity levels (Table 2 and Supplementary Table S5). At 17 °C, SFAs constituted only 27.6 % of TFAs. This proportion increased gradually, reaching 36.1 % at 29 °C and then surged to 52.7 % at 33 °C, nearly doubling the initial content observed at 17 °C. In contrast, PUFAs demonstrated an inverse trend. At 33 °C, PUFAs accounted for 25.8 % of TFAs, significantly lower than about 50 % and 60 % observed at 17 °C and 25 °C, respectively. Specific FAs also showed considerable variability across different temperatures. For example, the content of PA was around 21.0 % of TFAs at 25 °C but escalated to 34.6 % at 33 °C, making it the predominant FA. Stearic acid (SA, C18:0), typically present in trace amounts from 17 °C to 29 °C and across 19–34 ‰ salinity levels, notably increased to 8.2 % at 33 °C. EPA, usually one of the three dominant FAs at around 20 % of TFAs across all salinity levels and at temperatures up to 29 °C, declined to levels comparable to myristic acid (MA, C14:0), HDDA, HTA, and SA at 33 °C.

Prior research by Pahl et al. [28] examining the impact of temperature on the FAs of *C. cryptica* found that the FA profile remained relatively stable at 15 °C, 18 °C, and 25 °C. Our study, however, reveals a divergence from these findings, possibly due to our use of an autotrophic rather than a heterotrophic model for *C. cryptica* cultivation. Other diatom studies support our results, indicating that the saturation degree of FAs increases with rising temperature [52–54], thereby confirming that *C. cryptica* follows this general trend.

Similar to other diatom species, *C. cryptica* is rich in carotenoids such as fucoxanthin and diadinoxanthin. Guo et al. reported that *C. cryptica* had the highest biomass concentration and fucoxanthin content among 13 microalgal species from seven genera when grown under

Table 1
FAs and carotenoids composition of *C. cryptica* under different salinity levels.

	Salinity (‰)					
	19	22	25	28	31	34
Fatty acids (%TFAs)						
C14:0	8.5 ± 0.4	8.8 ± 0.5	9.2 ± 0.5	9.3 ± 0.7	8.8 ± 0.6	8.8 ± 0.7
C16:0	21.1 ± 1.0	20.2 ± 1.0	21.0 ± 0.2	20.3 ± 0.6	21.2 ± 0.3	20.8 ± 0.1
C16:1	19.7 ± 0.8	20.3 ± 0.6	19.9 ± 0.4	20.0 ± 0.6	20.7 ± 0.9	20.4 ± 0.6
C16:2	8.1 ± 0.6	7.9 ± 0.6	8.5 ± 0.9	7.7 ± 0.6	7.7 ± 0.6	7.8 ± 0.6
C16:3	9.5 ± 0.6^{b}	9.7 ± 0.5^{ab}	9.7 ± 0.3^{ab}	10.7 ± 0.7^{a}	9.6 ± 0.7^{ab}	9.5 ± 0.9^{b}
C18:0	0.8 ± 0.1	0.8 ± 0.0	0.8 ± 0.0	0.8 ± 0.0	0.8 ± 0.1	0.8 ± 0.0
C18:1	6.4 ± 0.7	6.0 ± 0.8	5.6 ± 0.9	5.5 ± 0.5	5.9 ± 0.3	5.9 ± 0.2
C18:2	0.8 ± 0.1^{c}	0.9 ± 0.1^{c}	1.0 ± 0.1^{bc}	1.6 ± 0.2^{a}	1.2 ± 0.2^{b}	1.1 ± 0.1^{bc}
C20:4	1.8 ± 0.3^{ab}	2.3 ± 0.3^{a}	1.4 ± 0.2^{b}	1.6 ± 0.1^{b}	1.4 ± 0.4^{b}	1.7 ± 0.4^{b}
C20:5	17.8 ± 0.6^{ab}	17.5 ± 0.4^{ab}	17.6 ± 0.9^{ab}	17.1 ± 0.4^{b}	18.1 ± 0.4^{ab}	18.5 ± 1.0^{a}
C22:6	5.5 ± 0.5^{a}	5.8 ± 0.3^{a}	5.4 ± 0.3^{a}	5.4 ± 0.3^{a}	4.6 ± 0.2^{b}	4.7 ± 0.4^{b}
SFAs	30.4 ± 1.1	29.7 ± 1.3	31.0 ± 0.5	30.3 ± 0.6	30.8 ± 0.9	30.4 ± 0.7
MUFAs	26.1 ± 1.4	26.3 ± 1.0	25.5 ± 1.3	25.6 ± 0.1	26.6 ± 0.9	26.4 ± 0.5
PUFAs	43.6 ± 1.0	44.0 ± 0.3	43.5 ± 1.6	44.1 ± 0.7	42.6 ± 0.7	43.2 ± 0.8
Carotenoids (mg g^{-1})						
Fucoxanthin	6.5 ± 0.9	6.9 ± 0.5	7.3 ± 0.4	6.9 ± 0.6	7.2 ± 0.3	7.0 ± 0.6
Diadinoxanthin	0.9 ± 0.0^{b}	0.7 ± 0.1^{b}	1.0 ± 0.1^{ab}	1.0 ± 0.2^{ab}	0.9 ± 0.0^{b}	1.2 ± 0.3^{a}

Note: Values are shown as mean ± SD (n = 3). TFAs, total fatty acids; SFAs, saturated fatty acids; MUFAs, monounsaturated fatty acids; PUFAs, polyunsaturated fatty acids. Values within the same column that share a common superscript letter indicate no significant difference, while groups denoted by non-overlapping superscript letters are considered significantly different (p < 0.05).

Table 2
FAs and carotenoids composition of *C. cryptica* under different temperature conditions.

	Temperature (°C)				
	17	21	25	29	33
C14:0	7.2 ± 0.5^{c}	9.2 ± 0.6^{ab}	9.2 ± 0.5^{ab}	8.7 ± 0.6^{b}	10.0 ± 0.2^{a}
C16:0	19.1 ± 0.5^{d}	21.3 ± 0.7^{c}	21.0 ± 0.2^{c}	26.0 ± 0.7^{b}	34.6 ± 0.8^{a}
C16:1	19.8 ± 0.5^{a}	19.3 ± 1.2^{a}	19.9 ± 0.4^{a}	19.0 ± 0.1^{a}	15.6 ± 0.8^{b}
C16:2	8.6 ± 0.3^{a}	8.0 ± 0.5^{a}	8.5 ± 0.9^{a}	6.7 ± 0.7^{b}	7.0 ± 0.3^{b}
C16:3	11.1 ± 0.8^{a}	8.9 ± 0.0^{b}	9.7 ± 0.3^{b}	12.1 ± 0.3^{a}	5.9 ± 0.9^{c}
C18:0	1.3 ± 0.4^{b}	0.9 ± 0.1^{bc}	0.8 ± 0.0^{c}	1.4 ± 0.2^{b}	8.2 ± 0.2^{a}
C18:1	4.0 ± 0.1^{b}	4.5 ± 0.7^{b}	5.6 ± 0.9^{ab}	5.0 ± 0.9^{ab}	5.8 ± 0.1^{a}
C18:2	3.9 ± 0.4^{b}	4.5 ± 0.3^{a}	1.0 ± 0.1^{c}	1.0 ± 0.3^{c}	1.2 ± 0.3^{c}
C20:4	1.9 ± 0.2^{b}	2.4 ± 0.1^{a}	1.4 ± 0.2^{c}	0.6 ± 0.1^{d}	0.8 ± 0.1^{d}
C20:5	19.3 ± 0.2^{a}	17.2 ± 0.6^{b}	17.6 ± 0.9^{b}	16.6 ± 0.9b	8.9 ± 0.6^{c}
C22:6	3.8 ± 0.2^{b}	3.9 ± 0.2^{b}	5.4 ± 0.3^{a}	2.8 ± 0.2^{c}	1.9 ± 0.2^{d}
SFAs	27.6 ± 0.4^{d}	31.4 ± 0.8^{c}	31.0 ± 0.5^{c}	36.1 ± 1.3^{b}	52.7 ± 0.9^{a}
MUFAs	23.8 ± 0.6^{b}	23.7 ± 1.8^{b}	25.5 ± 1.3^{a}	24.1 ± 0.9^{b}	21.5 ± 0.8^{b}
PUFAs	48.6 ± 0.2^{a}	44.9 ± 1.5^{b}	43.5 ± 1.6^{b}	39.8 ± 1.0^{c}	25.8 ± 1.5^{d}
Carotenoids (mg g^{-1})					
Fucoxanthin	4.8 ± 0.7^{b}	6.5 ± 0.1^{a}	7.3 ± 0.4^{a}	7.0 ± 0.7^{a}	2.5 ± 0.5^{c}
Diadinoxanthin	0.5 ± 0.2^{c}	0.9 ± 0.0^{b}	1.0 ± 0.1^{b}	1.1 ± 0.1^{b}	1.5 ± 0.2^{a}

Note: Values are displayed as mean ± SD (n = 3). TFAs, total fatty acids; SFAs, saturated fatty acids; MUFAs, monounsaturated fatty acids; PUFAs, polyunsaturated fatty acids. Values within the same column that share a common superscript letter indicate no significant difference, while groups denoted by non-overlapping superscript letters are considered significantly different (p < 0.05).

heterotrophic conditions [55]. Consistent with these findings [55,56], our results show that across all six salinity levels, *C. cryptica* maintained a stable fucoxanthin content of approximately 7.0 mg g^{-1} (Table 1 and Supplementary Table S4), and similar stability was observed for diadinoxanthin, with contents around 1.0 mg g^{-1} across the same salinity range. Interestingly, while diadinoxanthin content at 34 ‰ was significantly higher than at 22 ‰, there was no clear trend across varying salinity levels, and no significant differences were noted in fucoxanthin levels among the salinity groups. Within the temperature range of 21–29 °C, neither fucoxanthin nor diadinoxanthin levels showed significant variations (Table 2 and Supplementary Table S5). However, at the lower temperature of 17 °C, both carotenoids experienced substantial reductions, with levels approximately half those recorded at 25 °C. This observation aligns with the known response of microalgal cells to non-optimal temperatures, which can disrupt cellular energy equilibrium and lead to an overproduction of free radicals. To counteract these effects and promote survival, cells often increase the synthesis of pigments with antioxidant properties [14]. For instance, *Dunaliella salina* has been shown to ramp up β-carotene production under high temperatures [57]. In our study, while *C. cryptica* cultivated at 33 °C showed the lowest fucoxanthin levels (2.5 mg g^{-1}), it exhibited the highest diadinoxanthin levels (1.5 mg g^{-1}), suggesting that diadinoxanthin may play a more critical role in scavenging free radicals under thermal stress in this species.

3.3. Effects of salinity and temperature on the frustule properties of *C. cryptica*

The silica frustules of diatoms, characterized by their intricate patterning, large specific surface area, charged surfaces, outstanding thermal stability, and high absorbability, have garnered significant attention for various industrial applications, including drug delivery, hemostatic materials, microlenses, and biosensors [58]. *C. cryptica* exhibits a frustule structure composed of two centric valves interconnected by multiple girdle bands, resembling a petri dish-like configuration. Each valve consists of an external (distal) and an internal (proximal) face (Fig. 4a and a′). The proximal valve is distinguished by round, uniformly distributed cribrum pores arranged in radial patterns and separated by costae (Fig. 4b). Conversely, the distal valve features areolae structures (Fig. 4b′), which include relatively large, oval or elongated foramina and cribrum pores. Additionally, distinctive features such as rimoportulae on the valve rim and fultoportulae, comprising a central tube traversing the valve and three surrounding satellite pores, are prominently visible (Fig. 4c, d, c′, and d′). The morphological characteristics and physicochemical properties of these frustules are influenced by environmental parameters, impacting their potential effectiveness as biomaterials [59,60]. Understanding how cultivation conditions affect frustule phenotypes is therefore essential for optimizing their performance in targeted applications. This knowledge enables the strategic adjustment of

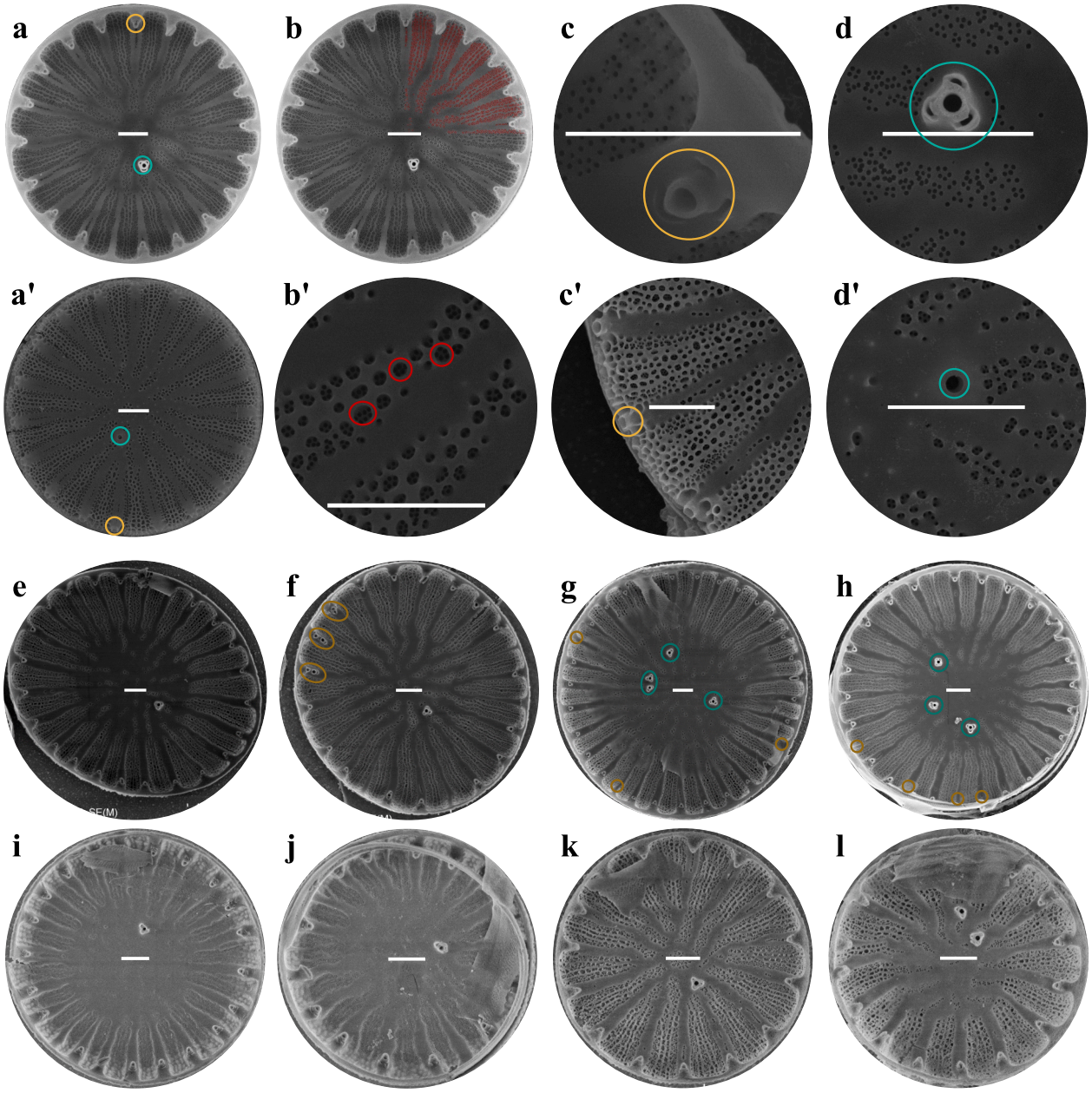

Fig. 4. SEM micrographs of proximal (a) and distal valve (a′), cribrum pores (b) and foramen structure (b′), rimoportula (c and c′), fultoportulae (d and d′), as well as valves under different salinity (e–h) and temperature (i–l) regimes. The cyan and yellow circles indicate fultoportulae and rimoportula, respectively, while the deep cyan and yellow circles (or ellipses) indicate abnormal fultoportulae and rimoportula, respectively. The red marks in panels b and b′ indicate cribrum pores and areolae structures, respectively. All scale bars are 1 μm. (For interpretation of the references to colour in this figure legend, the reader is referred to the web version of this article.)

growth parameters to consistently produce frustules with desired properties, enhancing their utility in various technological domains.

Salinity and temperature are critical environmental factors that significantly impact frustule phenotypes in diatoms, affecting characteristics such as valve outline, pore size, and biosilica content [61,62]. Despite their known importance, specific impacts of these factors on the frustules of *C. cryptica* have not been extensively studied. In our observations, variations in both salinity and temperature led to noticeable changes in the morphological properties and the degree of silicification of the valve. For example, at the extremities of the salinity range tested—17 ‰ and 34 ‰—valves (not all) appeared elliptical rather than the typical round shape (Fig. 4e and f). Furthermore, at higher salinity levels (31 ‰ and 34 ‰), we noted valves with multiple fultoportulae and abnormalities such as absent or redundant rimoportulae (Fig. 4f–h). Temperature also played a significant role in modifying frustule properties. At lower temperatures (17 °C and 21 °C), there was an enhanced degree of biosilicification, characterized by cribrum pores displaying reduced size and increased density (Fig. 4i and j). In contrast, at higher temperatures (29 °C and 33 °C), biosilica deposition seemed to be compromised, as evidenced by the presence of broken or interconnected cribrum pores (Fig. 4k and l).

To comprehensively assess the influence of salinity and temperature on the biosilicification process in *C. cryptica*, quantitative analyses were conducted on both cellular morphologies and biosilica content. Morphological characteristics were evaluated based on SEM micrographs, focusing on multiple parameters. In the context of salinity exposure, seven distinct morphological traits were measured: valve diameter, diameter and quantity of central fultoportulae, number of

costae, rimoportulae, and both the number and density of cribrum pores. However, the examination of temperature effects was confined to four morphological features—valve diameter, fultoportula number, costa number, and rimoportula number. This was due to the significant variability in the biosilica deposition of *C. cryptica* under different temperatures, which rendered parameters such as fultoportula diameter, cribrum pore number, and cribrum pore density difficult to identify accurately. Additionally, the biosilica content was quantitatively determined for all experimental treatments, facilitating a holistic understanding of environmental impacts on the biosilicification of *C. cryptica*.

As depicted in Fig. 5a, the valve diameter of *C. cryptica* demonstrated an incremental increase from 9.8 μm at a salinity of 19 ‰ to 12.5 μm at 34 ‰, indicating a positive correlation between valve diameter and salinity levels. While specific studies on the salinity and temperature impacts on valve diameter in *C. cryptica* have not been conducted previously, analogous research on *C. meneghiniana* and other diatoms offers valuable comparative perspectives. For instance, Roubeix and Lancelot reported significant reductions in both cell width (correlating with valve diameter) and height in *C. meneghiniana* with rising salinity levels [63]. Similarly, Aizdaicher and Markina observed a marked decline in cell height in *Corethron hystrix* with increased salinity, although the cell width remained stable across a salinity range of 16–32 ‰ [64]. *Thalassiosira pseudonana* displayed comparable trends, with cell height decreasing and cell width remaining constant under heightened salinity conditions [65]. In contrast, the present study recorded the highest valve diameter in *C. cryptica* at 34 ‰ (approximately 12.5 μm) and the lowest at 19 ‰ (approximately 9.8 μm), thereby showcasing a consistent increase in valve diameter with elevated salinity levels (Fig. 5a). This divergence from the patterns observed in previous studies suggests a distinctive frustule biogenesis response in *C. cryptica* to salinity variations. Additionally, the valve diameter of *C. cryptica* exhibited significant variability across different temperature conditions. Within a temperature spectrum of 17 °C to 33 °C, the valve diameter expanded

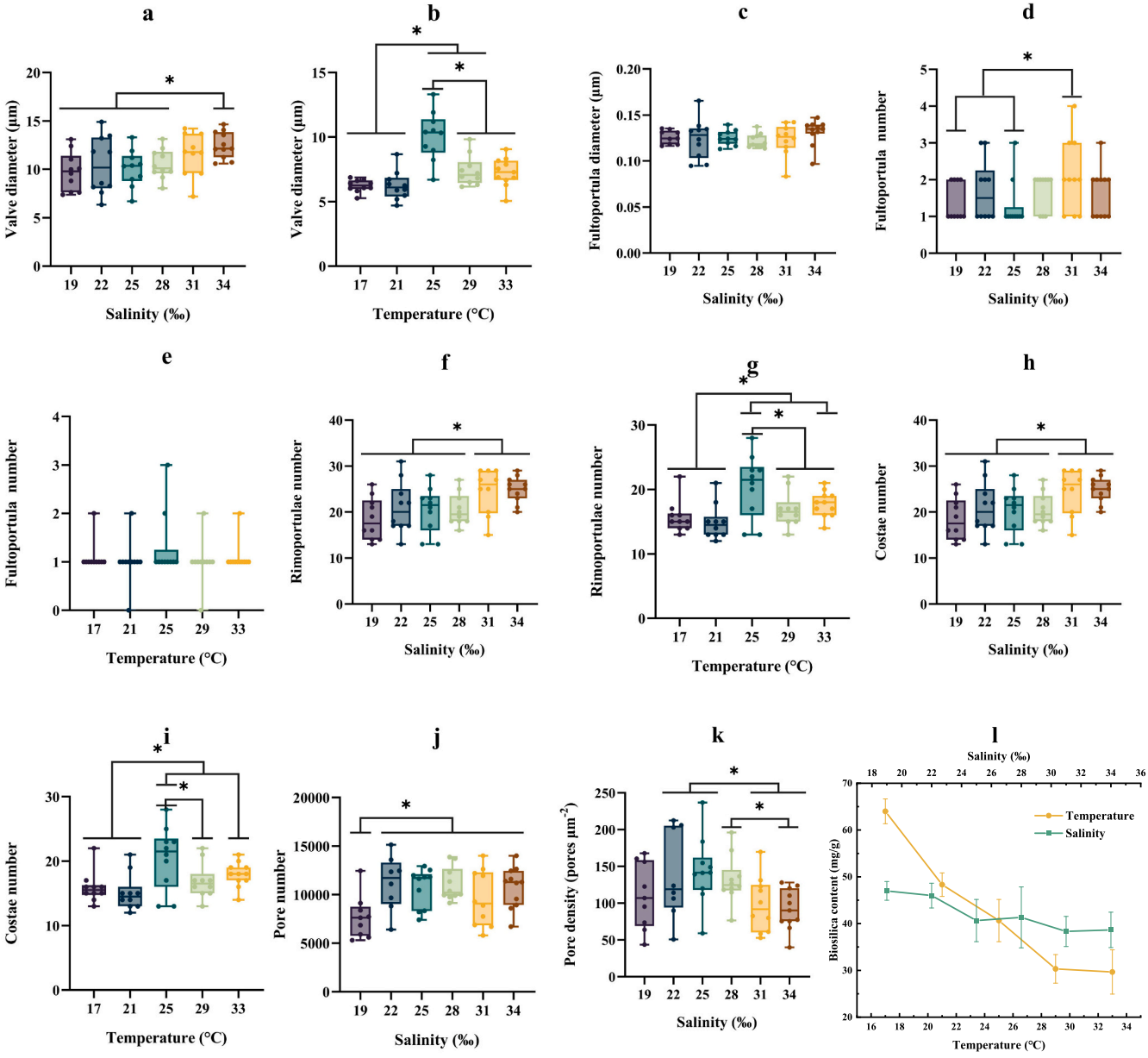

Fig. 5. Morphological properties (a–k) and biosilica content (h) of frustule under different salinity and temperature levels. Values are shown as mean ± SD (for a–k, $n = 8$–11; while for l, $n = 3$); * indicates significant differences ($p < 0.05$).

from 6.2 μm at 17 °C to 10.1 μm at 25 °C, before contracting to 7.3 μm at 33 °C, thus following a quadratic response pattern (Fig. 5b and Supplementary Table S6).

Fultoportulae and rimoportulae, structures intimately linked with the secretion of chitin fibrils that facilitate cell aggregation and buoyancy regulation, have been studied in several diatoms [66,67]. However, research into how environmental factors influence these structures shows no clear, consistent pattern. For instance, Shirokawa et al. observed an increased number of fultoportulae in *C. meneghiniana* when cultured in seawater compared to freshwater [67], while Håkansson and Chepurnov found only minor salinity-induced variations in fultoportula numbers in the same species [68]. Another study on *Thalassiosira decipiens* reported the absence or reduction of fultoportulae and rimoportulae at lower salinities (15 ‰ and 20 ‰), which was not observed at higher concentrations (25 ‰ and 30 ‰) [69]. In our current analysis, the diameter of fultoportulae across various salinity levels remained consistent at approximately 125.0 nm, with no significant differences detected among the groups (Fig. 5c and Supplementary Table S6). The greatest number of fultoportulae was noted at 31 ‰, significantly surpassing the counts at lower salinities (19 ‰ and 22 ‰). However, the variation in fultoportula numbers did not present a distinct pattern with salinity, as values at 28 ‰ and 34 ‰ resembled those at 19 ‰, 22 ‰, and 25 ‰ (Fig. 5d and Supplementary Table S6). The number of fultoportulae remained relatively stable across different temperature conditions, fluctuating between 1.0 and 1.3 (Fig. 5e). Regarding rimoportula numbers, a minimal count was observed at 19 ‰, increasing to a peak at 34 ‰, indicative of an upward trend with rising salinity (Fig. 5f). This structure exhibited a bell-shaped pattern across temperature treatments, diminishing at both the lower (17 °C and 21 °C) and higher (29 °C and 33 °C) temperature extremes (Fig. 5g). Moreover, the number of costae, typically corresponding one-to-one with rimoportula, mirrored the variation trends observed in rimoportula numbers under both salinity and temperature conditions (Fig. 5f–i).

Cribrum pores are essential for facilitating the exchange of substances between the internal cell environment and the external milieu, playing a pivotal role in the metabolic processes of diatoms [70]. Research indicates that the size of cribrum pores may adapt to salinity variations to sustain a consistent diffusive flux, thus enabling diatoms to assimilate comparable amounts of nutrients across different salinity levels [71]. Consequently, the dimension of cribrum pores has often been utilized as a critical metric to elucidate the impacts of environmental factors on frustule biogenesis. For example, Vrieling et al. observed a reduction in cribrum pore size in *Thalassiosira punctigera* and *T. weissflogii* under reduced salinity conditions [72], a trend similarly noted in other diatom species such as *Cocconeis placentula* and *Navicula salinarum* [73,74]. It is generally acknowledged that cribrum pore size increases with elevated salinity [62]. In this study, we shifted our focus to evaluating the number and density of cribrum pores in *C. cryptica* under varied salinities to derive new insights into cellular responses. As depicted in Fig. 5j, the minimum number of cribrum pores, approximately 7666 per valve, was recorded at a salinity of 19 ‰, which was significantly lower compared to other salinities tested. The peak value of approximately 11,196 pores per valve was observed at 22 ‰, with no notable differences among the salinity levels of 28 ‰, 31 ‰, and 34 ‰. Given the variation in valve diameter with salinity (Fig. 5a and Supplementary Table S6), which could influence the total number of cribrum pores, we also calculated cribrum pore density. As shown in Fig. 5k, the density of cribrum pores exhibited a peak of 143.8 pores per square micron at 19 ‰ and a low of 91.6 pores per square micron at 34 ‰, displaying an initial increase followed by a decrease across the salinity gradient from 19 ‰ to 34 ‰. Furthermore, while accurate quantification of cribrum pore number and density under varying temperature conditions proved challenging, SEM micrographs indicated that higher temperatures might facilitate an increase in these parameters, as evidenced in Fig. 4i–l. These findings underscore that *C. cryptica* appears capable of adjusting cribrum pore density in response to different salinity and temperature conditions.

Biosilica content, a crucial parameter for evaluating the extent of biosilicification, is extensively studied to elucidate the impacts of abiotic factors on frustule biogenesis. Despite extensive research, consensus on how various environmental factors influence biosilicification remains elusive. For instance, Tuchman et al. reported that *C. meneghiniana* exhibited reduced biosilica content at higher salinity levels [75], a finding subsequently corroborated by Olsen and Paasche in *Thalassiosira pseudonana* [76]. In contrast, McMillan and Johansen observed that *T. decipiens* grown under low salinity conditions showed decreased size and silicification compared to those in high salinity environments [69]. On the contrary, Roubeix and Lancelot found that cell silicification remained consistent across various salinity levels [63], while Vrieling et al. noted that *T. punctigera* and *T. weissflogii* developed denser, more hydrated biosilica under lower salinity [72]. In this study, we measured biosilica content relative to DCW to mitigate potential biases introduced by variations in valve size. As demonstrated in Fig. 5l and Supplementary Table S6, the biosilica content was highest at 19 ‰ (approximately 47.0 mg g^{-1} DCW) and 22 ‰ (around 46.0 mg g^{-1} DCW), both significantly exceeding values at other salinity levels, which ranged from 38.3 to 41.3 mg g^{-1} DCW. These findings align with those of Tuchman et al., Olsen and Paasche, and Vrieling et al., but differ from those of Roubeix and Lancelot, suggesting a decline in biosilicification with increasing salinity. Furthermore, additional studies indicate that temperatures surpassing the thermal optimum result in diminished silica production [44]. Consistently, the highest biosilica content in our study (64.0 mg g^{-1} DCW) was observed at 17 °C, while the lowest (30.3 mg g^{-1} DCW) occurred at 33 °C, indicating a linear decrease with rising temperatures.

3.4. Verification of transcriptional levels of silicalemma transmembrane proteins under different salinities

To substantiate the observation that the biosilicification process in *C. cryptica* diminishes with increasing salinity and temperature, we evaluated the transcriptional levels of genes involved in frustule biogenesis across various salinities and temperatures using RT-qPCR. Silaffins, which are well-documented for their involvement in biosilica deposition [77,78], have been difficult to identify in *C. cryptica* due to the absence of conserved amino acid sequences across diatom species. Consequently, our analysis included five silicalemma transmembrane proteins, some of which—or their homologs in *Thalassiosira pseudonana*—are known to significantly influence the microstructures and biosilica deposition within the frustules [78–80]. These assessments were conducted at three different time points: Days 4, 8, and 12.

Within different salinity conditions, transcriptional patterns of the five genes were clustered into three distinct groups (Fig. 6a–e). The first group, which includes *CcSin1*, *CcSAP2*, and *CcSAP3* (Fig. 6a, d, and e), displayed consistently reduced transcriptional levels across all three time points as salinity increased, indicating a strong sensitivity of these genes to salinity variations. The second group, represented by *CcSin2* (Fig. 6b), showed relatively stable transcriptional levels on Days 4 and 8, but experienced a decrease at Day 12 with increased salinity, suggesting a role in long-term adaptation to salinity. In contrast, *CcSin1*, *CcSAP2*, and *CcSAP3* may be implicated in both immediate and prolonged salinity responses [27]. The third group, comprised solely of *CcSAP1* (Fig. 6c), maintained stable transcriptional levels under all tested salinity regimes at all time points, suggesting minimal influence of salinity on its expression.

In terms of temperature impacts, dramatic fluctuations in the transcriptional levels of all five genes were noted across the temperature spectrum at all three time points (Fig. 6f–j). For instance, the transcriptional level of *CcSin1* at 17 °C was significantly higher—4.8, 9.5, and 26.8 times, respectively—than at 33 °C (Fig. 6f). Similarly, *CcSAP2* and *CcSAP3*, which are highly responsive to temperature, showed more than a 40-fold increase in transcription at 17 °C compared to 33 °C (Fig. 6i and j). Even *CcSAP1*, which exhibited stable transcription under

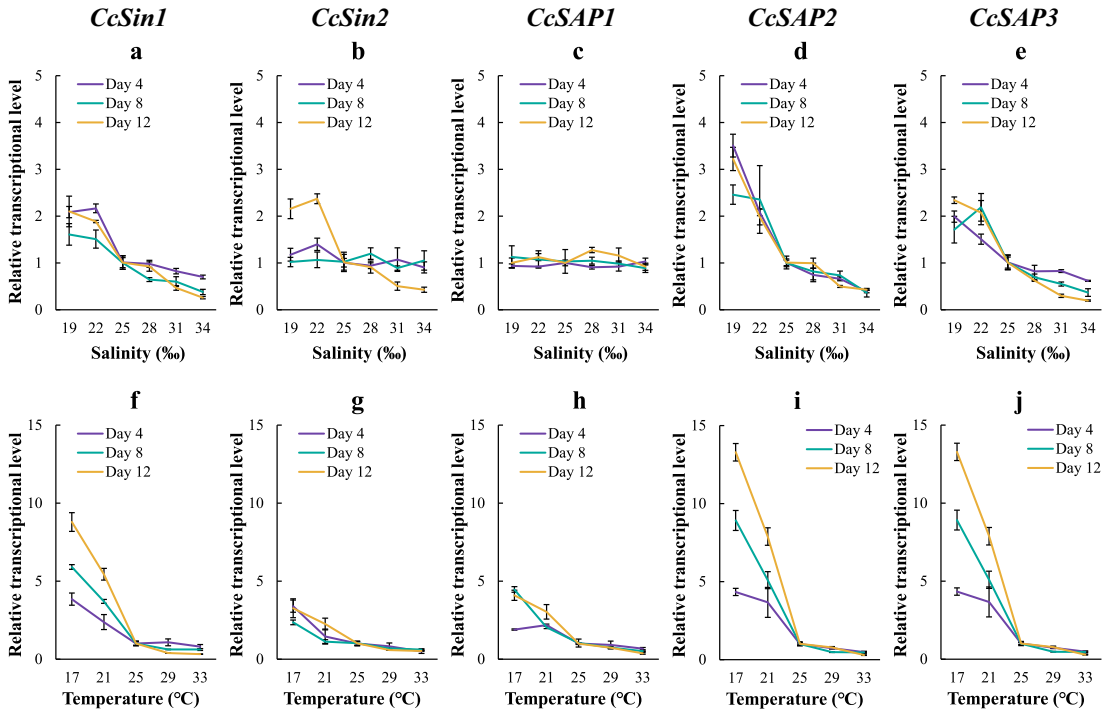

Fig. 6. Transcriptional abundances of genes associated with frustule biogenesis under different salinity (a–e) and temperature (f–j) levels. Values are presented as mean ± SD ($n = 3$); the groups at 25 ‰ salinity and 25 °C temperature serve as the control groups for the salinity and temperature treatments, respectively.

varying salinity levels, registered a substantial decrease in transcription with rising temperatures (Fig. 6h). These findings underscore the critical role that both salinity and temperature play in influencing biosilica deposition by modulating the transcription of genes associated with silicalemma transmembrane proteins.

4. Conclusions

This study comprehensively evaluated the effects of salinity and temperature on *C. cryptica*, demonstrating that salinities ranging from 19 ‰ to 34 ‰ exert minimal influence on the growth performance and biochemical composition of this diatom. Notably, the concentrations of fucoxanthin and EPA were consistent across the tested salinity levels, maintaining averages of approximately 7.0 mg g^{-1} of DCW and 18 % of TFAs, respectively. Additionally, *C. cryptica* exhibited robust survival across a broad temperature spectrum of 17 °C to 33 °C. However, temperatures at the extremities of this range (17 °C and 33 °C) impeded growth and induced significant alterations in macromolecular composition, FA profile, and carotenoid content. These findings underscore the remarkable adaptability of *C. cryptica* to environmental fluctuations, highlighting its potential for scaled-up cultivation in OPRs.

Furthermore, our analysis revealed that both salinity and temperature profoundly affect the biosilicification process in *C. cryptica*. Enhanced biosilica deposition correlated with increasing salinity and temperature, as supported by RT-qPCR analyses of genes associated with frustule biogenesis. Morphological adaptations were evident in increased valve diameter, rimoportula number, and costa number at higher salinities, whereas biosilica content inversely correlated with salinity. Cribrum pore density exhibited an increase from 19 ‰ to 25 ‰, followed by a decrease up to 34 ‰. Temperature impacts on biosilicification were marked by an initial increase and subsequent decrease in valve diameter, rimoportula number, and costa number with rising temperatures, while fultoportula number remained consistent across all temperatures. Moreover, a linear decline in biosilica content was observed with increasing temperature. Collectively, these results highlight the intricate interplay between environmental factors and the physiological and biochemical responses of *C. cryptica*, providing valuable insights for its cultivation and application perspectives in biotechnological sectors.

Supplementary data to this article can be found online at https://doi.org/10.1016/j.algal.2024.103751.

CRediT authorship contribution statement

Yicun Zhao: Writing – original draft, Methodology, Data curation. **Yan Sun:** Methodology, Formal analysis. **Zhengfeng Zhu:** Methodology, Formal analysis. **Lin Zhang:** Supervision, Investigation, Funding acquisition. **Jian Li:** Writing – review & editing, Formal analysis. **Spiros N. Agathos:** Writing – review & editing, Formal analysis. **Chengxu Zhou:** Writing – review & editing. **Jichang Han:** Writing – review & editing, Supervision, Resources, Funding acquisition.

Declaration of competing interest

The authors declare that they have no known competing financial interests or personal relationships that could have appeared to influence the work reported in this paper.

Acknowledgments

This work was supported by the Ningbo Public Welfare Science and Technology Program (2022S161), the National Natural Science Foundation of China (31902370), the Zhejiang Provincial Natural Science Foundation of China (LY22C190001), the Key Program of Science and Technology Innovation in Ningbo (2023Z118).

Data availability

Data will be made available on request.

References

[1] R. Mittal, V. Ranade, Bioactives from microalgae: a review on process intensification using hydrodynamic cavitation, J. Appl. Phycol. 35 (3) (2023) 1129–1161, https://doi.org/10.1007/s10811-023-02945-w.

[2] J. Joun, R. Sirohi, B.S. Yu, H.E. Yang, S.J. Sim, Utilizing wastewater and flue gas for enhancing biomass and high-value products from microalgae, Phytochem. Rev. 22 (4) (2023) 861–877, https://doi.org/10.1007/s11101-023-09876-x.

[3] M.I. Khan, J.H. Shin, J.D. Kim, The promising future of microalgae: current status, challenges, and optimization of a sustainable and renewable industry for biofuels, feed, and other products, Microb. Cell Factories 17 (1) (2018) 36, https://doi.org/10.1186/s12934-018-0879-x.

[4] Y. Pan, D.K. Amenorfenyo, M. Dong, N. Zhang, X. Huang, C. Li, F. Li, Effects of salinity on the growth, physiological and biochemical components of microalga *Euchlorocystis marina* [original research], Front. Mar. Sci. 11 (2024), https://doi.org/10.3389/fmars.2024.1402071.

[5] G.Q. Chen, Y. Jiang, F. Chen, Salt-induced alterations in lipid composition of diatom *Nitzschia laevis* (bacillariophyceae) under heterotrophic culture condition (1), J. Phycol. 44 (5) (2008) 1309–1314, https://doi.org/10.1111/j.1529-8817.2008.00565.x.

[6] M.G. de Morais, S. Vaz Bda, E.G. de Morais, J.A. Costa, Biologically active metabolites synthesized by microalgae, Biomed. Res. Int. 2015 (2015) 835761, https://doi.org/10.1155/2015/835761.

[7] A. Martínez-Roldán, H. Perales-Vela, R. Cañizares-Villanueva, G. Torzillo, Physiological response of *Nannochloropsis* sp. to saline stress in laboratory batch cultures, J. Appl. Phycol. 26 (2014) 115–121, https://doi.org/10.1007/s10811-013-0060-1.

[8] X. Duan, Salt-induced osmotic stress for lipid overproduction in batch culture of *Chlorella vulgaris*, Afr. J. Biotechnol. 11 (2012), https://doi.org/10.5897/AJB11.3670.

[9] M.L. Bartley, W.J. Boeing, A.A. Corcoran, F.O. Holguin, T. Schaub, Effects of salinity on growth and lipid accumulation of biofuel microalga *Nannochloropsis* salina and invading organisms, Biomass Bioenergy 54 (2013) 83–88, https://doi.org/10.1016/j.biombioe.2013.03.026.

[10] W. Wang, P. Yang, C. He, S. Chi, S. Li, K. Mai, F. Song, Effects of dietary methionine on growth performance and metabolism through modulating nutrient-related pathways in largemouth bass (Micropterus salmoides), Aquaculture Reports 20 (2021) 100642, https://doi.org/10.1016/j.aqrep.2021.100642.

[11] K. Kumar, S.K. Mishra, A. Shrivastav, M.S. Park, J.-W. Yang, Recent trends in the mass cultivation of algae in raceway ponds, Renew. Sust. Energ. Rev. 51 (2015) 875–885, https://doi.org/10.1016/j.rser.2015.06.033.

[12] S. Fon Sing, A. Isdepsky, M.A. Borowitzka, D.M. Lewis, Pilot-scale continuous recycling of growth medium for the mass culture of a halotolerant *Tetraselmis* sp. in raceway ponds under increasing salinity: a novel protocol for commercial microalgal biomass production, Bioresour. Technol. 161 (2014) 47–54, https://doi.org/10.1016/j.biortech.2014.03.010.

[13] M.J. Cooney, G. Young, R. Pate, Bio-oil from photosynthetic microalgae: case study, Bioresour. Technol. 102 (1) (2011) 166–177, https://doi.org/10.1016/j.biortech.2010.06.134.

[14] M. Ras, J.-P. Steyer, O. Bernard, Temperature effect on microalgae: a crucial factor for outdoor production, Rev. Environ. Sci. Biotechnol. 12 (2) (2013) 153–164, https://doi.org/10.1007/s11157-013-9310-6.

[15] P. Pérez-López, J.H. de Vree, G. Feijoo, R. Bosma, M.J. Barbosa, M.T. Moreira, R. H. Wijffels, A.J.B. van Boxtel, D.M.M. Kleinegris, Comparative life cycle assessment of real pilot reactors for microalgae cultivation in different seasons, Appl. Energy 205 (2017) 1151–1164, https://doi.org/10.1016/j.apenergy.2017.08.102.

[16] M. DuBois, K.A. Gilles, J.K. Hamilton, P.A. Rebers, F. Smith, Colorimetric method for determination of sugars and related substances, Anal. Chem. 28 (3) (1956) 350–356, https://doi.org/10.1021/ac60111a017.

[17] B.E.F. Reimann, J.M.C. Lewin, R.R.L. Guillard, *Cyclotella cryptica*, a new brackish-water diatom species, Phycologia 3 (2) (1963) 75–84, https://doi.org/10.2216/i0031-8884-3-2-75.1.

[18] S.M. Mitrovic, J.N. Hitchcock, A.W. Davie, D.A. Ryan, Growth responses of *Cyclotella meneghiniana* (Bacillariophyceae) to various temperatures, J. Plankton Res. 32 (8) (2010) 1217–1221, https://doi.org/10.1093/plankt/fbq038.

[19] J. Li, Y. Amano, M. Machida, Temperature-dependent growth characteristics and dominance trends of the cyanobacterium *Microcystis* sp. and the diatom *Cyclotella meneghiniana*, Hydrobiologia 849 (7) (2022) 1677–1688, https://doi.org/10.1007/s10750-022-04810-2.

[20] S.L. Pahl, D.M. Lewis, F. Chen, K.D. King, Heterotrophic growth and nutritional aspects of the diatom *Cyclotella cryptica* (Bacillariophyceae): effect of some environmental factors, J. Biosci. Bioeng. 109 (3) (2010) 235–239, https://doi.org/10.1016/j.jbiosc.2009.08.480.

[21] J. Fang, Y. Sun, Z. Zhu, J. Li, P. Cheng, S.N. Agathos, Y. Fu, L. Zhang, C. Zhou, J. Han, Algae-bacteria consortia promotes the cell growth of marine microalgae *Phaeodactylum tricornutum* and *Chrysotila roscoffensis*, Algal Res. 80 (2024) 103535, https://doi.org/10.1016/j.algal.2024.103535.

[22] K.M. Hsieh, L.W. Lion, M.L. Shuler, Bioreactor for the study of defined interactions of toxic metals and biofilms, Appl. Environ. Microbiol. 50 (5) (1985) 1155–1161, https://doi.org/10.1128/aem.50.5.1155-1161.1985.

[23] E.G. Bligh, W.J. Dyer, A rapid method of total lipid extraction and purification, Can. J. Biochem. Physiol. 37 (8) (1959) 911–917, https://doi.org/10.1139/o59-099.

[24] J.J. Sedmak, S.E. Grossberg, A rapid, sensitive, and versatile assay for protein using Coomassie brilliant blue G250, Anal. Biochem. 79 (1) (1977) 544–552, https://doi.org/10.1016/0003-2697(77)90428-6.

[25] Y. Sun, Y. Xin, L. Zhang, Y. Wang, R. Liu, X. Li, C. Zhou, L. Zhang, J. Han, Enhancement of violaxanthin accumulation in *Nannochloropsis oceanica* by overexpressing a carotenoid isomerase gene from *Phaeodactylum tricornutum*, Front. Microbiol. 13 (2022) 942883, https://doi.org/10.3389/fmicb.2022.942883.

[26] A.R. Kirkham, P. Richthammer, K. Schmidt, M. Wustmann, Y. Maeda, R. Hedrich, E. Brunner, T. Tanaka, K.H. van Pée, A. Falciatore, T. Mock, A role for the cell-wall protein silacidin in cell size of the diatom *Thalassiosira pseudonana*, ISME J. 11 (11) (2017) 2452–2464, https://doi.org/10.1038/ismej.2017.100.

[27] T. Nakov, K.J. Judy, K.M. Downey, E.C. Ruck, A.J. Alverson, Transcriptional response of osmolyte synthetic pathways and membrane transporters in a euryhaline diatom during long-term acclimation to a salinity gradient, J. Phycol. 56 (6) (2020) 1712–1728, https://doi.org/10.1111/jpy.13061.

[28] S.L. Pahl, D.M. Lewis, F. Chen, K.D. King, Heterotrophic growth and nutritional aspects of the diatom *Cyclotella cryptica* (Bacillariophyceae): effect of some environmental factors, J. Biosci. Bioeng. 109 (3) (2010) 235–239, https://doi.org/10.1016/j.jbiosc.2009.08.480.

[29] M.S. Liu, J.A. Hellebust, Effects of salinity and osmolarity of the medium on amino acid metabolism in *Cyclotella cryptica*, Can. J. Bot. 54 (9) (1976) 938–948, https://doi.org/10.1139/b76-098.

[30] S.H. Baek, S.W. Jung, K. Shin, Effects of temperature and salinity on growth of *Thalassiosira pseudonana* (Bacillariophyceae) isolated from ballast water, J. Freshw. Ecol. 26 (2011) 1–6, https://doi.org/10.1080/02705060.2011.582696.

[31] R. V, D. S, A. K, U. A, Isolation, identification, and optimization of growth conditions for the marine microalgae isolated from the Gulf of Mannar, south-east coast of India, Reg. Stud. Mar. Sci. 51 (2022) 102189, https://doi.org/10.1016/j.rsma.2022.102189.

[32] D.K. Khona, S.M. Shirolikar, K.K. Gawde, E. Hom, M.A. Deodhar, J.S. D'Souza, Characterization of salt stress-induced palmelloids in the green alga, *Chlamydomonas reinhardtii*, Algal Res. 16 (2016) 434–448, https://doi.org/10.1016/j.algal.2016.03.035.

[33] I. Ahmad, J.A. Hellebust, Osmoregulation in the extremely euryhaline marine micro-alga *Chlorella* autotrophica, Plant Physiol. 74 (4) (1984) 1010–1015, https://doi.org/10.1104/pp.74.4.1010.

[34] A. Kaçka, G. Dönmez, Isolation of *Dunaliella* spp. from a hypersaline lake and their ability to accumulate glycerol, Bioresour. Technol. 99 (17) (2008) 8348–8352, https://doi.org/10.1016/j.biortech.2008.02.042.

[35] M.S. Liu, J.A. Hellebust, Uptake of amino acids by the marine centric diatom *Cyclotella cryptica*, Can. J. Microbiol. 20 (8) (1974) 1109–1118, https://doi.org/10.1139/m74-173.

[36] M.S. Liu, J.A. Hellebust, Regulation of proline metabolism in the marine centric diatom *Cyclotella cryptica*, Can. J. Bot. 54 (9) (1976) 949–959, https://doi.org/10.1139/b76-099.

[37] J.C. Traller, S.J. Cokus, D.A. Lopez, O. Gaidarenko, S.R. Smith, J.P. McCrow, S. D. Gallaher, S. Podell, M. Thompson, O. Cook, M. Morselli, A. Jaroszewicz, E. E. Allen, A.E. Allen, S.S. Merchant, M. Pellegrini, M. Hildebrand, Genome and methylome of the oleaginous diatom *Cyclotella cryptica* reveal genetic flexibility toward a high lipid phenotype, Biotechnol. Biofuels 9 (2016) 258, https://doi.org/10.1186/s13068-016-0670-3.

[38] W.R. Roberts, K.M. Downey, E.C. Ruck, J.C. Traller, A.J. Alverson, Improved reference genome for *Cyclotella cryptica* CCMP332, a model for cell wall morphogenesis, salinity adaptation, and lipid production in diatoms (Bacillariophyta), G3 Genes|Genomes|Genetics 10 (9) (2020) 2965–2974, https://doi.org/10.1534/g3.120.401408.

[39] S. Sriharan, D. Bagga, M. Nawaz, The effects of nutrients and temperature on biomass, growth, lipid production, and fatty acid composition of *Cyclotella cryptica* Reimann, Lewin, and Guillard, Appl. Biochem. Biotechnol. 28 (1) (1991) 317–326, https://doi.org/10.1007/BF02922611.

[40] H. Thi Vu, S. Otsuka, H. Ueda, K. Senoo, Cocultivated bacteria can increase or decrease the culture lifetime of *Chlorella vulgaris*, J. Gen. Appl. Microbiol. 56 (5) (2010) 413–418, https://doi.org/10.2323/jgam.56.413.

[41] S.P. Singh, P. Singh, Effect of temperature and light on the growth of algae species: a review, Renew. Sust. Energ. Rev. 50 (2015) 431–444, https://doi.org/10.1016/j.rser.2015.05.024.

[42] J. Xia, Y. Bao, Y. Gao, J. Li, The effects of temperature and sulfamethoxazole on the growth and photosynthetic characteristics of *Phaeodactylum tricornutum*, Mar. Pollut. Bull. 200 (2024) 116122, https://doi.org/10.1016/j.marpolbul.2024.116122.

[43] H. Qiao, C. Cong, C. Sun, B. Li, J. Wang, L. Zhang, Effect of culture conditions on growth, fatty acid composition and DHA/EPA ratio of *Phaeodactylum tricornutum*, Aquaculture 452 (2016) 311–317, https://doi.org/10.1016/j.aquaculture.2015.11.011.

[44] C.E. Sheehan, K.G. Baker, D.A. Nielsen, K. Petrou, Temperatures above thermal optimum reduce cell growth and silica production while increasing cell volume and protein content in the diatom *Thalassiosira pseudonana*, Hydrobiologia 847 (20) (2020) 4233–4248, https://doi.org/10.1007/s10750-020-04408-6.

[45] P.G. Roessler, Changes in the activities of various lipid and carbohydrate biosynthetic enzymes in the diatom *Cyclotella cryptica* in response to silicon deficiency, Arch. Biochem. Biophys. 267 (2) (1988) 521–528, https://doi.org/10.1016/0003-9861(88)90059-8.

[46] S.P. Slocombe, Q. Zhang, M. Ross, A. Anderson, N.J. Thomas, Á. Lapresa, C. Rad-Menéndez, C.N. Campbell, K.D. Black, M.S. Stanley, J.G. Day, Unlocking nature's treasure-chest: screening for oleaginous algae, Sci. Rep. 5 (2015) 9844, https://doi.org/10.1038/srep09844.

[47] M.H. Huesemann, T.S. Hausmann, R. Bartha, M. Aksoy, J.C. Weissman, J. R. Benemann, Biomass productivities in wild type and pigment mutant of *Cyclotella*

sp. (diatom), Appl. Biochem. Biotechnol. 157 (3) (2009) 507–526, https://doi.org/10.1007/s12010-008-8298-9.
[48] S.M. Renaud, D.L. Parry, Microalgae for use in tropical aquaculture II: effect of salinity on growth, gross chemical composition and fatty acid composition of three species of marine microalgae, J. Appl. Phycol. 6 (3) (1994) 347–356, https://doi.org/10.1007/BF02181949.
[49] P.G. Kroth, A. Chiovitti, A. Gruber, V. Martin-Jezequel, T. Mock, M.S. Parker, M. S. Stanley, A. Kaplan, L. Caron, T. Weber, U. Maheswari, E.V. Armbrust, C. Bowler, A model for carbohydrate metabolism in the diatom *Phaeodactylum tricornutum* deduced from comparative whole genome analysis, PLoS One 3 (1) (2008) e1426, https://doi.org/10.1371/journal.pone.0001426.
[50] N.N. Zulu, K. Zienkiewicz, K. Vollheyde, I. Feussner, Current trends to comprehend lipid metabolism in diatoms, Prog. Lipid Res. 70 (2018) 1–16, https://doi.org/10.1016/j.plipres.2018.03.001.
[51] A. Cupo, S. Landi, S. Morra, G. Nuzzo, C. Gallo, E. Manzo, A. Fontana, G. d'Ippolito, Autotrophic vs., Heterotrophic cultivation of the marine diatom Cyclotella cryptica for EPA production, Mar. Drugs 19 (7) (2021), https://doi.org/10.3390/md19070355.
[52] A.A. Salamah, M.A. Ali, Effect of temperature on the lipid and fatty acid composition of *Yersinia pseudotuberculosis*, New Microbiol. 18 (1) (1995) 27–33.
[53] V. Pasquet, L. Ulmann, V. Mimouni, F. Guihéneuf, B. Jacquette, A. Morant-Manceau, G. Tremblin, Fatty acids profile and temperature in the cultured marine diatom *Odontella aurita*, J. Appl. Phycol. 26 (6) (2014) 2265–2271, https://doi.org/10.1007/s10811-014-0252-3.
[54] X. Shang, Y. Yang, Y. Zan, Z. Sun, Z. Lu, J. Sun, Effects of temperature on the growth, total lipid content and fatty acid composition of *Skeletonema dohrnii* [brief research report], Front. Mar. Sci. 11 (2024), https://doi.org/10.3389/fmars.2024.1361157.
[55] B. Guo, B. Liu, B. Yang, P. Sun, X. Lu, J. Liu, F. Chen, Screening of diatom strains and characterization of *Cyclotella cryptica* as a potential fucoxanthin producer, Mar. Drugs 14 (7) (2016), https://doi.org/10.3390/md14070125.
[56] C.R. Merz, N. Arora, M. Welch, E. Lo, G.P. Philippidis, Microalgal cultivation characteristics using commercially available air-cushion packaging material as a photobioreactor, Sci. Rep. 13 (1) (2023) 3792, https://doi.org/10.1038/s41598-023-30080-6.
[57] D.S. Pisal, S. Lele, Carotenoid production from microalga, *Dunaliella salina*, Indian J. Biotechnol. 4 (2005) 476–483.
[58] C. Yang, C. Feng, Y. Li, Z. Cao, Y. Sun, X. Li, L. Zhang, C. Zhou, J. Han, Morphological and physicochemical characteristics, biological functions, and biomedical applications of diatom frustule, Algal Res. 72 (2023) 103104, https://doi.org/10.1016/j.algal.2023.103104.
[59] Y. Su, N. Lundholm, M. Ellegaard, The effect of different light regimes on diatom frustule silicon concentration, Algal Res. 29 (2018) 36–40, https://doi.org/10.1016/j.algal.2017.11.014.
[60] L. Wang, Y. Sun, R. Zhang, K. Pan, Y. Li, R. Wang, L. Zhang, C. Zhou, J. Li, Y. Li, B. Zhu, J. Han, Enhancement of hemostatic properties of *Cyclotella cryptica* frustule through genetic manipulation, Biotechnol. Biofuels Bioprod. 16 (1) (2023) 136, https://doi.org/10.1186/s13068-023-02389-x.
[61] W. Fu, Y. Shu, Z. Yi, Y. Su, Y. Pan, F. Zhang, S. Brynjolfsson, Diatom morphology and adaptation: current progress and potentials for sustainable development, Sustainable Horizons. 2 (2022) 100015, https://doi.org/10.1016/j.horiz.2022.100015.
[62] Y. Su, N. Lundholm, M. Ellegaard, Effects of abiotic factors on the nanostructure of diatom frustules—ranges and variability, Appl. Microbiol. Biotechnol. 102 (14) (2018) 5889–5899, https://doi.org/10.1007/s00253-018-9087-1.
[63] V. Roubeix, C. Lancelot, Effect of salinity on growth, cell size and silicification of an euryhaline freshwater diatom. *Cyclotella meneghiniana* Kutz, Transitional Waters Bulletin. 2 (2008) 31–38, https://doi.org/10.1285/i1825229Xv2n1p31.
[64] N.A. Aizdaicher, Z.V. Markina, The effect of decrease in salinity on the dynamics of abundance and the cell size of *Corethron Hystrix* (Bacillariophyta) in laboratory culture, Ocean Science Journal. 45 (1) (2010) 1–5, https://doi.org/10.1007/s12601-010-0001-8.
[65] M. Hildebrand, E. York, J.I. Kelz, A.K. Davis, L.G. Frigeri, D.P. Allison, M. J. Doktycz, Nanoscale control of silica morphology and three-dimensional structure during diatom cell wall formation, J. Mater. Res. 21 (10) (2006) 2689–2698, https://doi.org/10.1557/jmr.2006.0333.
[66] P. LeDuff, G.L. Rorrer, Formation of extracellular β-chitin nanofibers during batch cultivation of marine diatom *Cyclotella* sp. at silicon limitation, J. Appl. Phycol. 31 (6) (2019) 3479–3490, https://doi.org/10.1007/s10811-019-01879-6.
[67] Y. Shirokawa, K. Karino, S. Mayama, Developmental plasticity and genotype–environment interactions influence valve morphology in the *Cyclotella meneghiniana* species complex (Bacillariophyceae), Eur. J. Phycol. 47 (3) (2012) 245–253, https://doi.org/10.1080/09670262.2012.697580.
[68] H. Håkansson, V. Chepurnov, A study of variation in valve morphology of the diatom *Cyclotella meneghiniana* in monoclonal cultures: effect of auxospore formation and different salinity conditions, Diatom Res. 14 (2) (1999) 251–272, https://doi.org/10.1080/0269249X.1999.9705469.
[69] M. McMillan, J.R. Johansen, Changes in valve morphology of *Thalassiosira decipiens* (Bacillariophyceae) cultured in media of four different salinities, Br. Phycol. J. 23 (4) (1988) 307–316, https://doi.org/10.1080/00071618800650341.
[70] S. Leterme, A. Ellis, J. Mitchell, M.-J. Buscot, T. Pollet, M. Schapira, L. Seuront, Morphological flexibility of *Cocconeis placentula* (Bacillariophyceae) nanostructure to changing salinity levels, J. Phycol. 46 (2010) 715, https://doi.org/10.1111/j.1529-8817.2010.00850.x.
[71] L. Chen, X. Men, M. Ma, P. Li, Q. Jiao, S. Lu, F. Kong, S. Wu, Polysaccharide release by aphanothece halophytica inhibits cyanobacteria/clay flocculation, J. Phycol. 46 (2010) 417–423, https://doi.org/10.1111/j.1529-8817.2010.00826.x.
[72] E.G. Vrieling, Q. Sun, M. Tian, P.J. Kooyman, W.W.C. Gieskes, R.A. van Santen, N. A.J.M. Sommerdijk, Salinity-dependent diatom biosilicification implies an important role of external ionic strength, Proc. Natl. Acad. Sci. 104 (25) (2007) 10441–10446, https://doi.org/10.1073/pnas.0608980104.
[73] H.A. McManus, L.A. Lewis, E.T. Schultz, Distinguishing multiple lineages of *Pediastrum duplex* with morphometrics and a proposal for lacunastrum gen. nov (1), J. Phycol. 47 (1) (2011) 123–130, https://doi.org/10.1111/j.1529-8817.2010.00941.x.
[74] E. Vrieling, L. Poort, T. Beelen, W. Gieskes, Growth and silica content of the diatoms *Thalassiosira weissflogii* and *Navicula salinarum* at different salinities and enrichments with aluminum, Eur. J. Phycol. 34 (1999) 307–316, https://doi.org/10.1080/09670269910001736362.
[75] M.L. Tuchman, E. Theriot, E.F. Stoermer, Effects of low level salinity concentrations on the growth of *Cyclotella meneghiniana* Kütz. (Bacillariophyta), Arch. Protistenkd. 128 (4) (1984) 319–326, https://doi.org/10.1016/S0003-9365(84)80003-2.
[76] S. Olsen, E. Paasche, Variable kinetics of silicon-limited growth in *Thalassiosira pseudonana* (Bacillariophyceae) in response to changed chemical composition of the growth medium, Br. Phycol. J. 21 (2) (1986) 183–190, https://doi.org/10.1080/00071618600650211.
[77] N. Poulsen, N. Kröger, Silica morphogenesis by alternative processing of silaffins in the diatom *Thalassiosira pseudonana*, J. Biol. Chem. 279 (41) (2004) 42993–42999, https://doi.org/10.1074/jbc.M407734200.
[78] M. Hildebrand, S. Lerch, R. Shrestha, Understanding diatom cell wall silicification—moving forward, Front. Mar. Sci. 5 (2018), https://doi.org/10.3389/fmars.2018.00125.
[79] A. Kotzsch, P. Gröger, D. Pawolski, P.H.H. Bomans, N. Sommerdijk, M. Schlierf, N. Kröger, Silicanin-1 is a conserved diatom membrane protein involved in silica biomineralization, BMC Biol. 15 (1) (2017) 65, https://doi.org/10.1186/s12915-017-0400-8.
[80] B. Tesson, S.J.L. Lerch, M. Hildebrand, Characterization of a new protein family associated with the silica deposition vesicle membrane enables genetic manipulation of diatom silica, Sci. Rep. 7 (1) (2017) 13457, https://doi.org/10.1038/s41598-017-13613-8.